



# Elevating adipose eosinophils in obese mice to physiologically normal levels does not rescue metabolic impairments

W. Reid Bolus<sup>1</sup>, Kristin R. Peterson<sup>2</sup>, Meria J. Hubler<sup>1</sup>, Arion J. Kennedy<sup>1</sup>, Marnie L. Gruen<sup>1</sup>, Alyssa H. Hasty<sup>1,3,\*</sup>

## ABSTRACT

**Objective:** Obesity is a metabolic disorder that has reached epidemic proportions worldwide and leads to increased risk for diabetes, cardiovascular disease, asthma, certain cancers, and various other diseases. Obesity and its comorbidities are associated with impaired adipose tissue (AT) function. In the last decade, eosinophils have been identified as regulators of proper AT function. Our study aimed to determine whether normalizing the number of AT eosinophils in obese mice, to those of lean healthy mice, would reduce obesity and/or improve metabolic fitness.

**Methods:** C57BL/6J mice fed a high fat diet (HFD) were simultaneously given recombinant interleukin-5 (rIL5) for 8 weeks to increase AT eosinophils. Metabolic fitness was tested by evaluating weight gain, AT inflammation, glucose, lipid, and mixed-meal tolerance, AT insulin signaling, energy substrate utilization, energy expenditure, and white AT being capacity.

**Results:** Eosinophils were increased ~3-fold in AT of obese HFD-fed mice treated with rIL5, and thus were restored to levels observed in lean healthy mice. However, there were no significant differences in rIL5-treated mice among the above listed comprehensive set of metabolic assays, despite the increased AT eosinophils.

**Conclusions:** We have shown that restoring obese AT eosinophils to lean healthy levels is not sufficient to allow for improvement in any of a range of metabolic features otherwise impaired in obesity. Thus, the mechanisms that identified eosinophils as positive regulators of AT function, and therefore systemic health, are more complex than initially understood and will require further study to fully elucidate.

Published by Elsevier GmbH. This is an open access article under the CC BY-NC-ND license (<http://creativecommons.org/licenses/by-nc-nd/4.0/>).

**Keywords** Inflammation; Obesity; Diabetes; Eosinophils; Interleukin 5; Adipose tissue

## 1. INTRODUCTION

Eosinophils are white blood cells classically associated with clearing parasitic infections and mediating immune reactions such as allergy and asthma. The characteristic appearance of an eosinophil is marked by its multi-lobular nucleus and granule-rich cytoplasm. Like many leukocytes, eosinophils develop in the bone marrow and migrate through the blood to infiltrate tissues in response to potent cytokines and chemokines, such as eotaxin 1, 2, and 3; IL-5; GM-CSF; and RANTES [1]. Eosinophils can synthesize an array of chemokines, cytokines, and lipid mediators; these aid in their ability to regulate tissue damage [2,3], wound healing [4], the onset of estrus [5], mammary

gland development [6], GI tract remodeling [7], and T-cell proliferation, polarization, and apoptosis [8,9]. Thus, eosinophils are versatile immune cells that contribute to their local environment in a tissue-specific manner.

Perhaps one of the most unexpected new roles identified for eosinophils is their potential influence on whole-body metabolic fitness by regulating adipose tissue (AT) health. Eosinophils were first discovered to reside in AT in 2011 by Wu *et al* [10]. In this paper, an eosinophil-deficient mouse model ( $\Delta$ dblGATA) was more susceptible to weight gain on a high fat diet (HFD), had impaired systemic glucose tolerance, greater AT insulin resistance, and fewer M2-like anti-inflammatory macrophages, which are all potential signs of AT

<sup>1</sup>Department of Molecular Physiology and Biophysics, Vanderbilt University School of Medicine, Nashville, TN, 37232, USA <sup>2</sup>Department of Pharmacology, Vanderbilt University School of Medicine, Nashville, TN, 37232, USA <sup>3</sup>VA Tennessee Valley Healthcare System, Nashville, TN, 37212, USA

\*Corresponding author. Room 702 Light Hall, Nashville, TN, 37232-0615, USA. Fax: +1 615 322 8973. E-mail: [alyssa.hasty@vanderbilt.edu](mailto:alyssa.hasty@vanderbilt.edu) (A.H. Hasty).

**Abbreviations:** AT, adipose tissue; HFD, high fat diet; rIL5, recombinant interleukin 5 protein; GM-CSF, Granulocyte-macrophage colony-stimulating factor; RANTES, Regulated on Activation, Normal T Cell Expressed and Secreted; ILC2, type 2 innate lymphoid cell; IL33, interleukin 33; IL25, interleukin 25; IL4, interleukin 4; IL13, interleukin 13; IP, intraperitoneal; MMPC, Mouse Metabolic Phenotyping Center; PFA, paraformaldehyde; FBS, fetal bovine serum; LP, lamina propria; EL, epithelial layer; DAPI, 4',6-diamidino-2-phenylindole; PI, propidium iodide; FCSR, flow cytometry shared resource; CISR, cell imaging shared resource; TG, triglycerides; FFA, free fatty acids; HA&ASC, hormone assay and analytical services core; RT, room temperature; Mme, metabolically active macrophages; eAT, epididymal AT; sAT, subcutaneous AT; pAKT, phosphorylated AKT; Ucp1, uncoupling protein 1; CCR2, C–C motif chemokine receptor 2

Received November 3, 2017 • Revision received December 2, 2017 • Accepted December 8, 2017 • Available online 16 December 2017

<https://doi.org/10.1016/j.molmet.2017.12.004>

dysfunction. In contrast, hypereosinophilic IL-5tg mice had reduced weight and improved glucose tolerance. Since this study, a series of papers have further elucidated the role of eosinophils in AT [11–18]. It has been shown that eosinophils accumulate in AT in response to IL5 produced by ILC2 cells when activated by IL33 and/or IL25. AT eosinophils can then produce IL4 and/or IL13 to yield a more M2-like polarization of the macrophage pool, which is typically associated with better AT health [19].

To date, interventional studies have targeted eosinophils via non-specific means (e.g. helminth infection, IL25/IL33 injections, cold-exposure) [10–17], which increase eosinophils but also alter a cascade of upstream or off-target immune reactions; thus, making it difficult to definitively conclude eosinophils are responsible for the observed improvements in metabolic fitness. Studies that directly targeted eosinophils were genetic mouse models that exhibit altered eosinophil content throughout gestational and post-natal development, making it unclear if metabolic improvements were developmental in origin [10,18]. Our current study aimed to determine whether directly normalizing AT eosinophil numbers via rIL5 injections in obese mice, after normal development has occurred, would have a similar effect (*i.e.* improved metabolic fitness) as seen in previous models that did not control for these factors. In our current study, AT eosinophils of obese mice were successfully restored to levels of lean mice with rIL5 treatment, but none of the metabolic improvements seen in other hypereosinophilic models were observed. We conclude that emerging paradigms suggesting eosinophils improve AT function, and thus systemic metabolic health, will need further study to fully understand the role of eosinophils in metabolic disease.

## 2. MATERIALS AND METHODS

### 2.1. Animals

C57BL/6J male wild type mice were purchased from the Jackson Laboratory (Bar Harbor, Maine) at 7 weeks of age and housed in the animal facility at Vanderbilt University for 1 week to acclimate. At 8 weeks of age, mice either remained on chow diet or were given *ad libitum* access to HFD with 60% kcal from fat (Research Diets, New Brunswick, NJ) for 8 weeks. During the entire 8-week period, mice also received 50 ng recombinant IL5 (rIL5; R&D Systems, Minneapolis, MN) protein (in 0.001% BSA as carrier protein) by intraperitoneal (IP) injection twice per week to elevate eosinophils. Carrier protein 0.001% BSA (vehicle) and saline injections were tested separately as controls (Figure 1A). Approximately 60% of mice responded to the 50 ng dose of rIL5 with increased eosinophils, as defined by greater than 1 standard deviation above the mean of saline controls. With our goal of studying mice with elevated eosinophils, only mice identified as responders were analyzed. Body composition was measured to obtain lean mass and fat mass by nuclear magnetic resonance (NMR) using a Bruker Minispec instrument (Woodlands, TX) in Vanderbilt's Mouse Metabolic Phenotyping Center (MMPC). Given that metabolic assays can be demanding on mice, multiple cohorts of mice were used to carry out the variety of metabolic experiments described below. Circulating blood was removed by perfusing the left ventricle of the heart with ~10–15 mL PBS. Individual tissues were then removed, weighed, and either snap-frozen in liquid nitrogen, fixed in 10% formalin, fixed in 1% PFA, or processed to isolate immune cells, in preparation for later analysis. Vanderbilt's Institutional Animal Care and

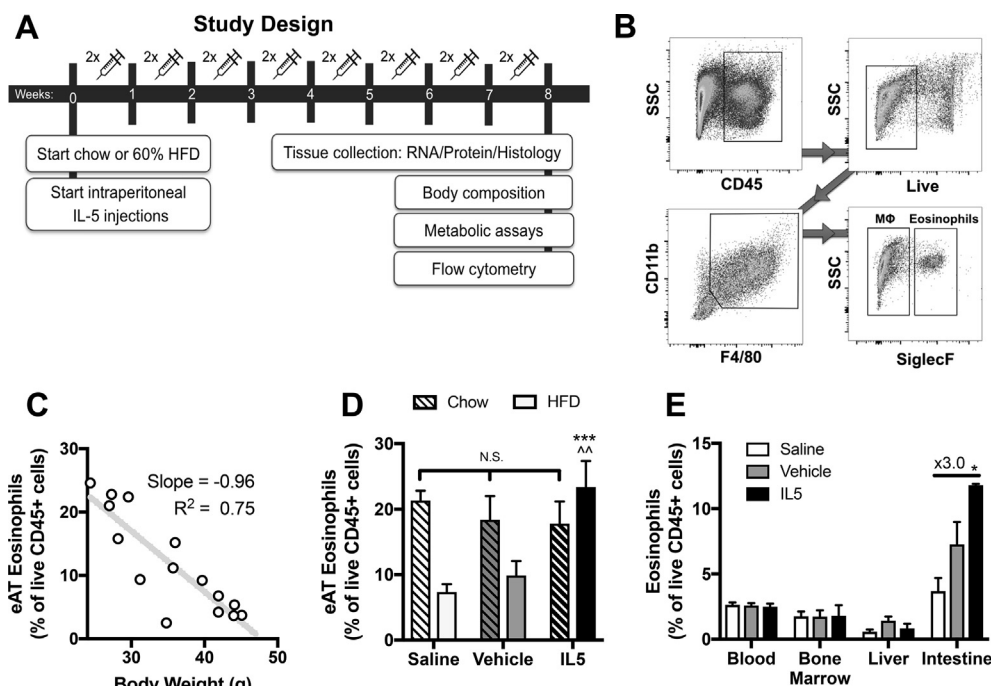


**Figure 1: Eosinophil levels in eAT, blood, bone marrow, liver, and intestine of rIL5 injected mice.** (A) Male C57BL/6J mice were fed either chow or HFD for 8 weeks and simultaneously IP injected twice weekly with rIL5 protein. (B) Flow cytometry gating strategy for eosinophils (CD45<sup>+</sup>, live, F4/80<sup>lo</sup>, CD11b<sup>lo</sup>, SiglecF<sup>+</sup>) and macrophages (CD45<sup>+</sup>, live, F4/80<sup>hi</sup>, CD11b<sup>hi</sup>, SiglecF<sup>-</sup>). (C) Percent eAT eosinophils negatively correlate with body weight (slope = -0.96, R<sup>2</sup> = 0.75). (D) Treatment with rIL5 elevates eAT eosinophils in HFD-fed mice, compared to saline and vehicle controls, back to chow-fed levels [n = 4–11]. (E) No difference in percent eosinophils in blood, bone marrow, or liver of rIL5 treated mice, but intestine does show an increase [n = 2–8]. Data are shown as means ± SEM. eAT = epididymal adipose tissue; HFD = high fat diet. Key: chow = hashed bars; HFD = open bars; saline = white; vehicle = grey; rIL5 = black. \*P < 0.05, compared to saline; \*\*\*P < 0.0005, compared to saline; ^^P < 0.005, compared to vehicle.

Use Committee approved all animal procedures prior to their implementation.

## 2.2. Immune cell isolation and flow cytometry

**AT stromal vascular fraction cell isolation:** AT was excised and minced into fine pieces in a 1% FBS PBS solution. Minced AT was digested with 2 mg/mL type II collagenase for 40 min at 37 °C at 200 rpm rotation (MaxQ4450, Thermo Fisher Scientific, Middletown, VA). PBS with 1% FBS solution was added to dilute the collagenase solution 4-fold. Solution was vortexed and passed through a 100 µm filter. After centrifugation, the cell pellet was treated with ACK lysis buffer to remove red blood cells. Reaction was neutralized by dilution with 1% FBS PBS, centrifuged, and decanted; cell pellet was resuspended and used for further analysis.

**Liver non-parenchymal cell isolation:** Liver was excised and minced in 1 mg/mL type II collagenase in 3% FBS PBS solution. Minced liver was incubated at 37 °C for 30 min at 200 rpm rotation (MaxQ4450). Cell suspension was filtered through a 100 µm filter and centrifuged at 300 rpm for 3 min (Sorvall ST 40R, Thermo Fisher Scientific). Supernatant was collected and centrifuged at 1500 rpm for 10 min. Pellet was resuspended in 40% Percoll and overlaid on top of 60% Percoll. Percoll gradient was centrifuged at 2000 rpm for 20 min. The two middle layers of the Percoll gradient were collected in 3% FBS in RPMI and centrifuged at 1500 rpm for 10 min. Supernatant was discarded; cell pellet was resuspended and stained for flow cytometry.

**Small intestine immune cell isolation:** Intestine between stomach and cecum was excised and cleaned of fat and Payer's patches. Fecal matter was removed by flushing with PBS. Intestine was cut longitudinally and mucus was gently scraped away with forceps. Intestine was cut into 1 cm pieces and cleaned of remaining mucus by vigorous shaking with PBS in a 50 mL conical tube. Pieces were incubated in dissociation media [1x HBSS (Ca/Mg-free), 5 mM EDTA, and 10 mM HEPES] for 20 min at 37 °C at 200 rpm rotation to separate lamina propria (LP) from epithelial layer (EL) (Sorvall ST 40R). Mixture was vortexed vigorously and passed through a 100 µm filter. Supernatant was collected as EL fraction, while remaining tissue in filter was collected and finely minced for a LP fraction. LP fraction was incubated in digestion solution [10% FBS, 2 mg/mL (250 U/mL) type IV collagenase, DMEM] for 20 min at 37 °C at 200 rpm rotation (MaxQ4450); then supernatant was passed through a 100 µm filter. LP fraction tissue was digested, filtered a second time, and LP supernatants were combined. EL and LP fractions were pelleted, resuspended in a 40% Percoll solution, centrifuged, and decanted; cell pellet was resuspended and used for further analysis.

**Bone marrow cell isolation:** Tibia and femur bones were removed and cleaned of tissue. Ends of bones were cut and flushed with RPMI. Collected marrow was passed through a 27-gauge needle several times slowly to create a single cell suspension. After centrifugation and decantation, the cell pellet was treated with ACK lysis buffer to remove red blood cells. Reaction was neutralized by dilution with 1% FBS PBS, centrifuged, and decanted; cell pellet was resuspended and used for further analysis.

**Blood cell isolation:** Approximately 200 µL blood was collected retro-orbitally in heparinized capillary tubes. Blood was diluted with 2 mL deionized water in a 15 mL conical tube and mixed by inverting for 15 s to lyse red blood cells. Reaction was neutralized by dilution with 10 mL 1% FBS PBS, centrifuged, and decanted; cell pellet was resuspended and used for further analysis.

**Flow cytometric analysis:** Isolated immune cells were first incubated with Fc Block (BD Biosciences, San Jose, CA) for ≥5 min on ice. Cells

were stained for 30 min at 4 °C, while protected from light, with a combination of fluorophore-conjugated antibodies: F4/80: APC (eBiosciences, Waltham, MA), CD11b: FITC/APC-Cy7/APC (BD Biosciences), SiglecF: PE/BV450 (BD Biosciences), CD45: PE-Cy7 (BD Biosciences), APC-Cy7/BV605 (Biolegend), CD3: FITC (BD Biosciences), TCRβ: APC-Cy7 (BD Biosciences), CD4: A700 (BD Biosciences), CD8: FITC/V500 (BD Biosciences), CD19: APC-Cy7 (BD Biosciences), Ly6C: FITC (BD Biosciences), Ly6G: PE (BD Biosciences), MHCII: FITC (BD Biosciences). Cells were washed several times, counting beads added, and stained with viability dye, [1 µg/mL 4',6-diamidino-2-phenylindole (DAPI) or propidium iodide (PI)], just before flow cytometric analysis. Cells were analyzed on a 4-laser BD LSR Fortessa (BD Biosciences) in the Vanderbilt Flow Cytometry Shared Resource (FCSR). Results were analyzed using FlowJo software.

## 2.3. RNA isolation, cDNA synthesis, and real-time RT-PCR

The Qiagen RNeasy Mini Kit was used to isolate RNA according to the manufacturer's instructions, after tissues were initially homogenized in TRIzol (BD Biosciences). Purified RNA was reverse transcribed by iScript RT (Bio-Rad, Hercules, CA) into cDNA. Differences in relative gene expression were quantified using FAM-conjugated TaqMan Gene Expression Assay (Life Technologies). Data were normalized to the housekeeping gene, 18s, and analyzed by the Pfaffl method [20].

## 2.4. Immunohistochemistry

**Eosinophil and macrophage detection in whole AT:** Small pieces of whole AT were fixed in 1% PFA for 1 h with agitation. AT was washed several times in PBS with agitation and stored in PBS at 4 °C until further processing. AT was cut into ~3 mm<sup>3</sup> pieces and incubated overnight at 4 °C with slow agitation in anti-mouse SiglecF-PE (BD Biosciences) and anti-mouse F4/80-APC (eBiosciences) at a 1:50 dilution. The next day, samples were washed in PBS, incubated with 1 µg/mL DAPI (BD Biosciences) for 3 min at RT with agitation, and rinsed with PBS. Samples were imaged on an Olympus FV-1000 confocal inverted microscope available through the Vanderbilt Cell Imaging Shared Resource (CISR). Each image stack spanned ~30 microns (1 image/1 micron) and was then compiled into a single 3D rendering using Imaris software.

## 2.5. Glucose tolerance test

Mice were fasted for 6 h during the light cycle. Fasting blood glucose levels were read using an ACCU-CHEK Aviva Plus glucometer (Roche, Basel, Switzerland) via the tail vein after a small tail clip. A 20% glucose solution was administered IP at 2 mg/kg lean mass, followed by blood glucose readings at 15, 30, 45, 60, 90, and 120 post glucose dosing.

## 2.6. Triglyceride tolerance test

Mice were fasted overnight for 16 h to deplete liver glycogen stores and induce lipolysis. Blood was collected via the tail vein after a small tail clip to measure fasting triglycerides (TG), free fatty acids (FFA), glucose, and cholesterol. Mice received an oral gavage of olive oil at 200 µL/mouse, and additional blood was collected for analysis at 1, 2, 3, 4, and 5 h after gavage.

## 2.7. Ad libitum mixed-meal tolerance test

Mice were fasted overnight for 16 h. Blood was collected via the tail vein after a small tail clip to measure fasting glucose, insulin, TG, FFA, and cholesterol. Mice were refed up to 1.5 g HFD *ad libitum* and additional blood was collected for analysis at 0.5, 1, 2, and 3 h after refeeding.

### 2.8. Plasma insulin

Insulin was measured by the Vanderbilt Hormone Assay and Analytical Services Core (HA&ASC) via radioimmunoassay using a double antibody procedure. Final analysis was accomplished by quantifying bound radioactive counts with a Packard Gamma counter connected to a computerized data reduction station.

### 2.9. Plasma lipids

FFAs were measured from mouse serum using a Cell Biolabs FFA Assay Kit via the manufacturer's instructions (Cell Biolabs, San Diego, CA). TGs were measured from mouse serum using an Infinity TG Assay Kit via the manufacturer's instructions (Thermo Fisher Scientific). Cholesterol was measured from mouse serum using an Infinity Cholesterol Assay Kit via the manufacturer's instructions (Thermo Fisher Scientific).

### 2.10. Insulin signaling

Mice were fasted for 6 h, given an IP insulin dose of 1 U/kg according to total body weight, and sacrificed 15 min later. Tissues were snap frozen in liquid nitrogen. Protein was extracted by homogenization in lysis buffer (20 mM Tris HCL, 150 mM NaCl, 1 mM EDTA, 1 mM EGTA, 0.5% NP-40, 2.5 mM Sodium Pyrophosphate, 1 mM Sodium Orthovanadate, 0.5 mM PMSF, 2% SDS). Insulin signaling was detected via western blotting by probing for phosphorylated-AKT (1:1000) vs. total AKT (1:1000) (Cell Signaling).

### 2.11. Energy expenditure and cold challenge

Mice were placed in metabolic cages at Vanderbilt's MMPC for 2 days at 21 °C room temperature (RT) followed by 2 days at 4 °C. The temperature flux took approximately 1 h to reach 4 °C. Body weight, food and water consumption, oxygen and carbon dioxide levels, and movement were all measured continuously throughout the duration of the 4-day study.

### 2.12. Statistics

All statistical graphs and analyses were performed in GraphPad Prism 7.0 software. Statistical tests include: student's *t*-test, one-way ANOVA with a Holm-Sidak *post-hoc* test for multiple comparisons, and two-way ANOVA with a Holm-Sidak *post-hoc* test for multiple comparisons. Outliers were removed by the ROUT method, with  $Q = 5\%$ . Significance was defined by a *P* value of  $\leq 0.05$ .

## 3. RESULTS

### 3.1. Eosinophil levels in AT, blood, bone marrow, liver, and intestine of rIL5 injected mice

Male C57BL/6J mice were fed either chow or HFD for 8 weeks and simultaneously injected twice weekly with rIL5 protein as depicted in Figure 1A. AT eosinophils were identified as CD45<sup>+</sup>, F4/80<sup>+</sup>, CD11b<sup>lo</sup>, SiglecF<sup>+</sup> (Figure 1B), as previously reported [10,21]. Replicating the literature, we report the percent eosinophils in AT decline with increased body weight; slope =  $-0.96$ ,  $R^2 = 0.75$  (Figure 1C). Despite the decline in AT eosinophils with weight gain on HFD, obese mice injected with rIL5 had increased eosinophils compared to vehicle injected controls, representing a physiological restoration to AT eosinophil percentages observed in lean mice (Figure 1D; chow-fed mice = hashed bars, HFD-fed mice = solid bars). In both circulating blood and at the site of eosinophil origin in the bone marrow, eosinophils were not increased with rIL5 (Figure 1E). In the liver, another metabolically relevant tissue to obesity, there was no change in the percent of eosinophils (Figure 1E). However, in eosinophil-

enriched intestine, a 3x-fold increase in eosinophils was noted in rIL5 treated animals (Figure 1E,  $P = 0.0298$ ). Slight changes in some other immune cell populations were observed in blood and liver but not in bone marrow or intestine (Supp. Figure 1).

### 3.2. Inflammatory profile of obese AT with elevated eosinophils

Typical epididymal AT (eAT) inflammation of moderate obesity was seen in both saline and vehicle controls, with classic crown-like structures of macrophages encompassing dead or dying adipocytes (Figure 2A). AT of rIL5 treated mice retained macrophages but also revealed an abundance of eosinophils throughout the tissue (Figure 2A). In addition to cell surface markers (F4/80<sup>+</sup> macrophages, SiglecF<sup>+</sup> eosinophils), these cell types can be further verified via nuclear morphology with a spherical nucleus in macrophages and a donut-shaped or multi-lobed nucleus in eosinophils. The percent of adipose macrophages increased by 24% in HFD-fed obese mice compared to lean mice (data not shown), a typical trend observed during weight gain. However, in the eAT stromal vascular fraction between treatment groups in HFD-fed obese mice, there were no significant differences in the percent macrophages (Figure 2B) or protein expression of pro-inflammatory M1-like marker, MHCII (Figure 2C). Likewise, whole eAT gene expression analysis of macrophage marker, *Adgre1* (F4/80), was not statistically different between groups (Figure 2D). An assortment of macrophage polarization genes, including pro-inflammatory M1-like markers (*Tnf*, *Il1 $\beta$* ), metabolically active Mme markers (*Tnf*, *Il1 $\beta$* , *Plin2*, *Abca1*), and anti-inflammatory M2-like markers (*Clec10a*, *Arg1*, *Retnla*, *Chil3*) showed no difference with vehicle- or rIL5-treatment (Figure 2D). Though AT eosinophils were increased with rIL5 treatment, there was no change in *Il13* gene expression, an M2-polarizer that can be secreted by eosinophils (Figure 2D). This may account for the lack of change in the AT macrophage percentage and polarization. Gene expression of another M2-polarizer, *Il4*, was also examined but was not detected at reliably sufficient levels to report.

### 3.3. Weight gain, body composition, and glucose tolerance in mice with elevated AT eosinophils

We next determined whether restoration of adipose eosinophils could reduce weight gain, modulate body composition, and/or improve glucose tolerance. Typical of diet-induced obesity, vehicle HFD-fed mice gained more weight ( $\sim 7$  g) than their vehicle chow-fed counterparts (Figure 3A and B). However, rIL5 did not reduce the total weight gain in mice on HFD (Figure 3B). Likewise, vehicle-treated mice gained proportionally more fat mass while on HFD than chow-fed, but rIL5 did not blunt this effect (Figure 3C and D). Specifically, eAT and subcutaneous AT (sAT) expanded in mass equally in vehicle- and rIL5-treated mice while on HFD, with no difference in liver weight at this duration of diet (Figure 3E). Glucose tolerance tests showed an expected impairment of both fasting blood glucose and systemic glucose tolerance in HFD-fed mice compared to chow-fed mice, but the increased AT eosinophils from 8 weeks of rIL5 injections did not improve glucose tolerance (Figure 3F).

### 3.4. Triglyceride tolerance in mice with elevated AT eosinophils

Fasted mice were challenged with an oral gavage of olive oil to determine whether increased eosinophils impact AT function by changing uptake of dietary fats. Following fat gavage, plasma TGs peaked between 2 and 3 h in both vehicle- and rIL5-treated mice (Figure 4A). Plasma FFAs also peaked at  $\sim 2$  h in both groups (Figure 4B). There was no difference in blood glucose (Figure 4C) or plasma cholesterol (Figure 4D) between groups.

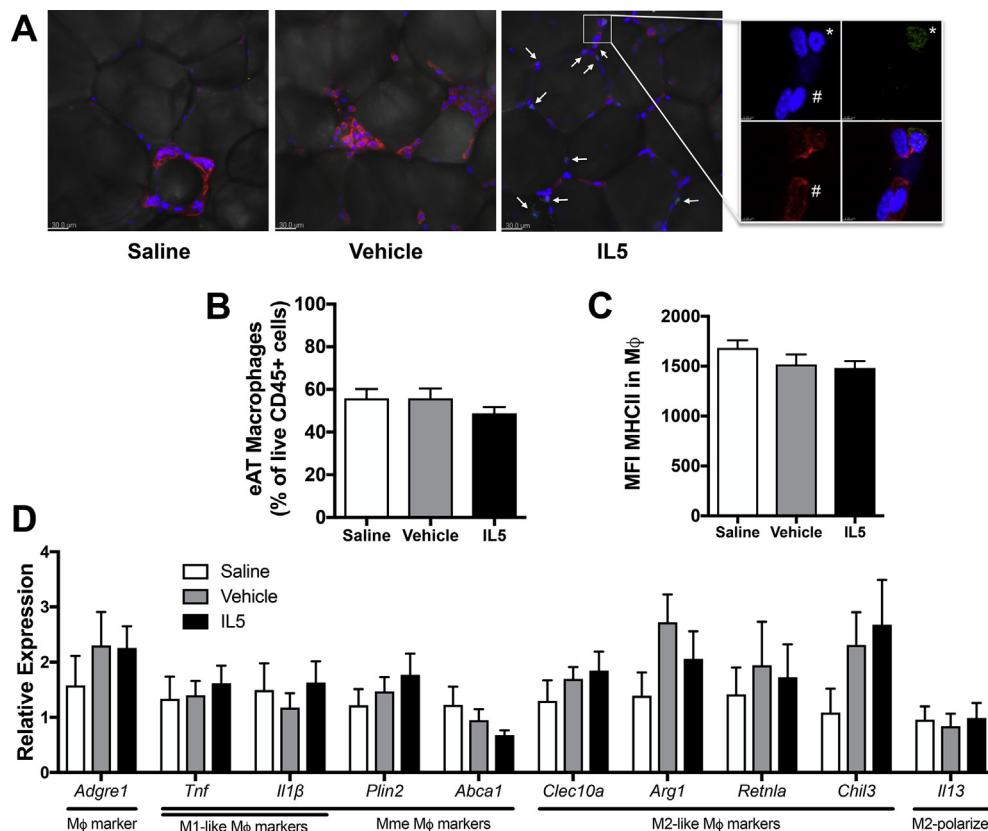


**Figure 2: Inflammatory profile of obese eAT with elevated eosinophils.** (A) Representative 40× images of eAT from HFD-fed obese mice treated with saline, vehicle, or rIL5. Macrophages (red, F4/80) are seen in abundance in all groups, whereas eosinophils (green, SiglecF) are increased in rIL5 treated mice. Magnified view shows the donut-shaped nucleus (\*) of eosinophils juxtaposed to the spherical nucleus (#) of macrophages [n = 3]. (B) Treatment with rIL5 does not alter percent eAT macrophages or (C) protein expression of pro-inflammatory marker MHCII [n = 6–11]. (D) Gene expression analysis of macrophage marker, *Adgre1* (F4/80), and an array of macrophage polarization genes were not statistically different between groups in eAT [n = 6–8]. Data are shown as means ± SEM. eAT = epididymal adipose tissue, HFD = high fat diet. Key: saline = white; vehicle = grey; rIL5 = black.

### 3.5. Metabolic parameters of rIL5 treated mice during a mixed-meal test

Fasted mice were given access to HFD *ad libitum* for 3 h to determine any differences in food consumption or metabolic parameters in response to elevated AT eosinophils. Both groups consumed the same amount of food, ~0.65 g, during the first 3 h of refeeding (Figure 5A). Upon refeeding, blood glucose levels increased and peaked at 0.5 h with a slow decline thereafter, but with no difference in mice with increased AT eosinophils compared to control (Figure 5B). Correspondingly, insulin levels increased alongside glucose levels (Figure 5C). Similar to the TG tolerance test (Figure 4), both TGs (Figure 5D) and FFAs (Figure 5E) took several hours to peak and then returned to baseline by the last time point (3 h), but with no difference among groups. Plasma cholesterol did not vary between groups (Figure 5F). There were no differences in basal fasting levels of any of the metabolic parameters measured (Figure 5).

### 3.6. Insulin signaling in AT with elevated eosinophils

The ratio of phosphorylated AKT (pAKT) to total AKT was assessed as a readout of tissue-specific insulin sensitivity. As expected, the ratio of pAKT/AKT from AT was increased in vehicle-treated mice upon insulin stimulation (Figure 6A and B). Though the AT pAKT/AKT ratio from rIL5-

treated mice also increased with insulin stimulation, there was no difference compared to control (Figure 6A and B).

### 3.7. Cold challenge: energy balance in mice with elevated eosinophils

Mice were individually housed in metabolic cages to measure an array of sensitive physiological parameters for 4 days. The second half was spent in 4 °C to determine any differences in energy balance while under a demanding stress on AT function. The average daily body weight was similar between vehicle- and rIL5-treated mice (Figure 7A). Average daily food intake (Figure 7B) and movement (Figure 7C) were increased in the dark cycle compared to the light cycle as expected, but with no difference among groups. Even before cold induction, the respiratory quotient for both groups was closer to 0.7 than 1.0, indicative of the high fat content from the HFD being used as a primary energy source (Figure 7D). Upon cold exposure, both groups continue to modulate their ratio of carbs/fats as a fuel source in the same manner with no significant differences at any time point (Figure 7D). Energy expenditure fluxes were higher during the dark cycle than the light cycle for both groups equally, at both RT and cold (Figure 7E). Upon cold exposure, rIL5-treated mice increase their energy expenditure to maintain body heat at the same rate as control mice

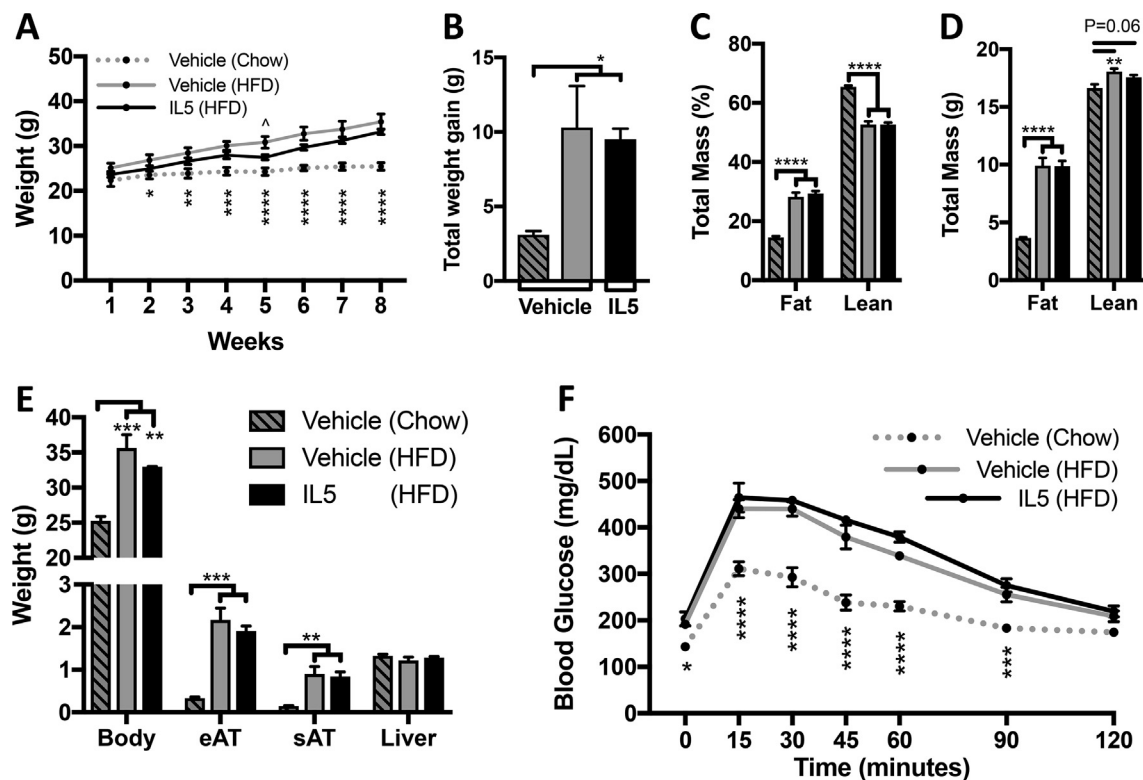


**Figure 3: Weight gain, body composition, and glucose tolerance in mice with elevated AT eosinophils.** (A) HFD-fed mice gained more weight over 8 weeks compared to chow, with no difference in (B) total weight gained between vehicle or rIL5 treated mice [ $n = 4$ ]. HFD-fed vehicle and rIL5 treated mice have equally altered total fat and lean mass by (C) percent or (D) grams at study completion [ $n = 4-12$ ]. (E) HFD-fed mice have increased body, eAT, and sAT weight, but no further difference with rIL5 [ $n = 4$ ]. (F) Glucose tolerance is impaired by HFD-feeding, but not rescued by rIL5 treatment [ $n = 4$ ]. Data are shown as means  $\pm$  SEM. AT = adipose tissue; HFD = high fat diet; eAT = epididymal AT; sAT = subcutaneous AT. Key: chow = hashed bars, dotted lines; HFD = open bars, solid lines; vehicle = grey; rIL5 = black. \* $P < 0.05$ , compared to chow; \*\* $P < 0.005$ , compared to chow; \*\*\* $P < 0.0005$ , compared to chow; \*\*\*\* $P < 0.0001$ , compared to chow;  $\wedge P < 0.005$ , compared to vehicle.

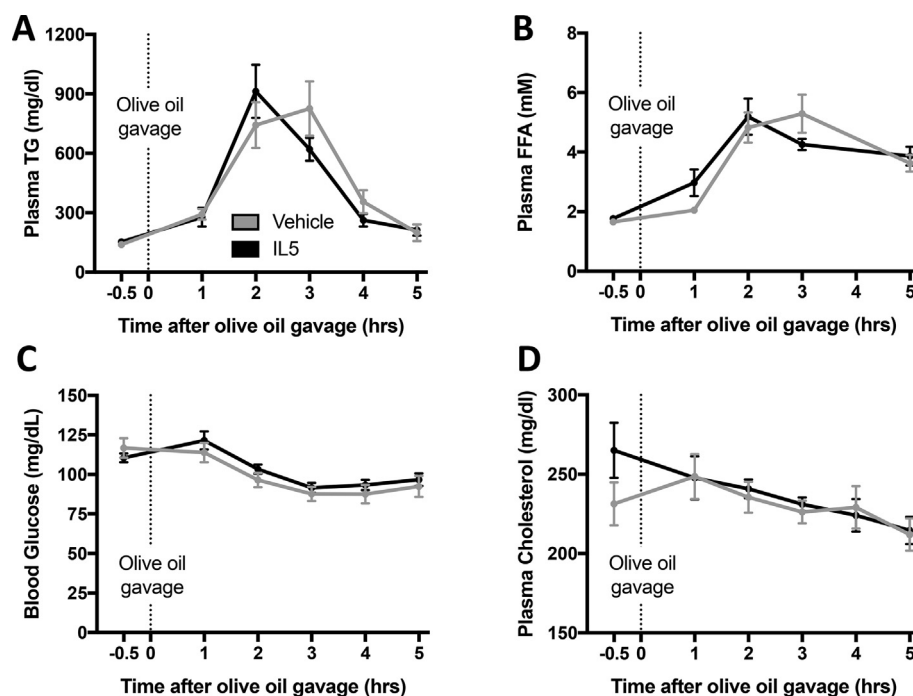


**Figure 4: Triglyceride tolerance in mice with elevated AT eosinophils.** Fasted HFD-fed mice treated with vehicle or rIL5 for 8 weeks were given a bolus of TGs (i.e. olive oil) and showed no difference between groups in (A) plasma TG [ $n = 8$ ] (B) plasma FFA [ $n = 4$ ] (C) blood glucose [ $n = 8$ ] (D) or plasma cholesterol [ $n = 8$ ] over the course of 5 h. Data are shown as means  $\pm$  SEM. HFD = high fat diet; TG = triglycerides; FFA = free fatty acids. Key: vehicle = grey; rIL5 = black.

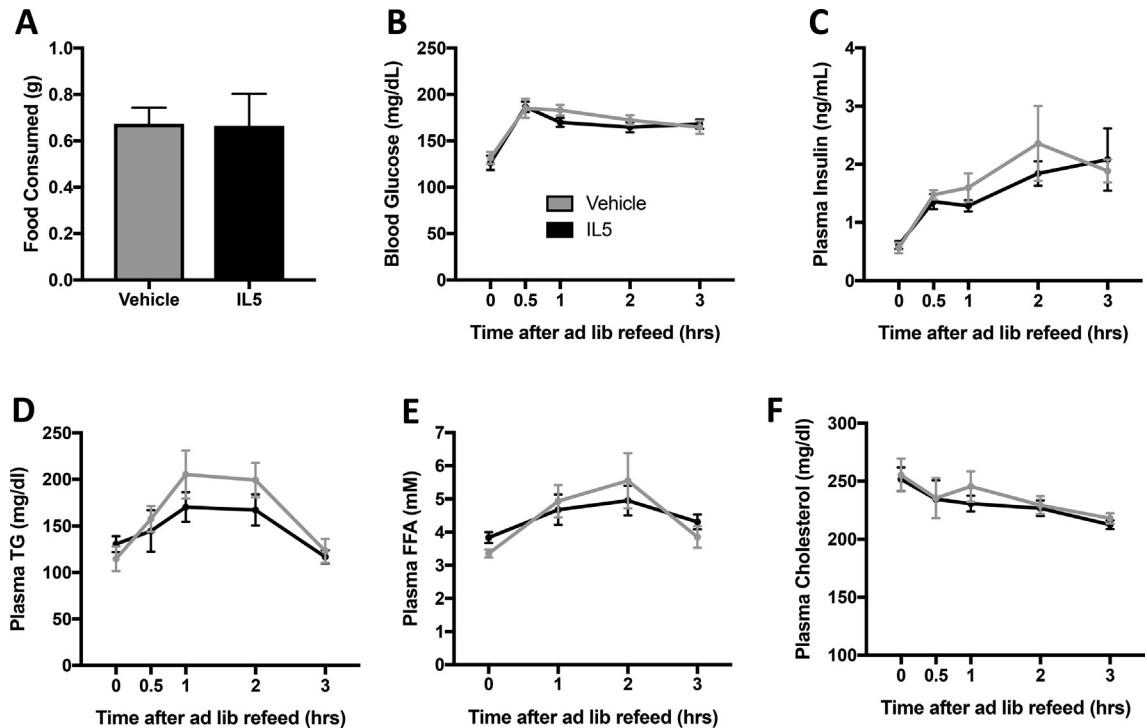


**Figure 5: Metabolic parameters of rIL5 treated mice during a mixed-meal test.** HFD-fed mice treated with vehicle or rIL5 for 8 weeks were fasted and then allowed access to HFD *ad libitum* for 3 h. (A) Both groups consumed the same amount of food [n = 6–7]. (B) A spike in blood glucose occurred at 0.5 h following refeeding with no difference between groups [n = 6–7]. (C) Insulin also rose at 0.5 h and then held relatively steady in both groups [n = 6–7]. Plasma (D) TG [n = 6–7], (E) FFA [n = 4], and (F) cholesterol [n = 5–7] did not vary between groups upon refeeding. Data are shown as means  $\pm$  SEM. HFD = high fat diet; TG = triglycerides; FFA = free fatty acids. Key: vehicle = grey; rIL5 = black.

(Figure 7E). The amount of total body mass (Figure 7F), fat mass (Figure 7G), and lean mass (Figure 7H) lost during cold exposure was not significantly different between groups.

### 3.8. Cold challenge: being capacity of white AT with elevated eosinophils

AT of mice subjected to 48 h 4 °C cold exposure was examined for indication of being, the process of white AT accruing the energy burning phenotype of brown AT. Eosinophil levels were examined after cold exposure, because published work has shown a correlation between cold-exposure and the amount of AT eosinophils [13,15]. Indeed, sAT eosinophils increased with cold exposure (Figure 8A) with

a further increase in sAT eosinophils in rIL5-treated mice. Indicative of an initiated being response, sAT *Ucp1* gene expression was significantly increased  $\sim$ 307-fold in cold-exposed mice compared to mice housed at RT (Figure 8B); however, there was no further increase in *Ucp1* in rIL5 treated mice despite the increased eosinophils. In eAT, eosinophils did not increase upon cold exposure but did respond to rIL5 with  $\sim$ 3.2-fold increase in their numbers (Figure 8C). Gene expression of *Ucp1* trended towards an increase with cold exposure but displayed no additive effect with rIL5 treatment (Figure 8D).

## 4. DISCUSSION

The major finding from this study was that restoring naturally occurring eosinophil numbers in AT, otherwise compromised by diet-induced obesity, is not sufficient to reestablish metabolic fitness. Administration of rIL5 was effectively used to elevate AT eosinophils during 8 weeks of HFD feeding (Figure 1). Of note, eosinophils were not modulated until mice had undergone normal development and reached adulthood. Equally important, eosinophils of obese AT were restored with rIL5 to physiologically relevant levels observed in lean AT, not super-physiological levels seen in previous models. Despite restoring obese AT eosinophils, there were no effects on AT inflammation (Figure 2), weight gain (Figure 3), glucose or lipid tolerance (Figures 3–5), insulin sensitivity (Figure 6), energy substrate utilization (Figure 7), energy expenditure (Figure 7), or AT being capacity (Figure 8). Though this set of metabolic parameters of AT health is not exhaustive, it is quite comprehensive. Thus, it is unlikely an effect of restoring AT eosinophils in obese mice on metabolic output was overlooked.

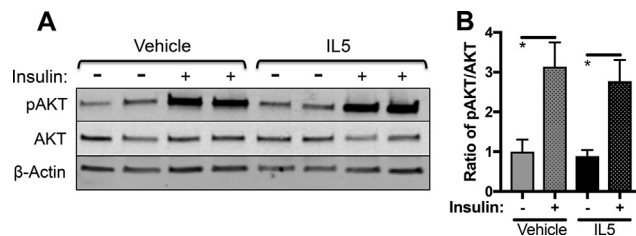


**Figure 6: Insulin signaling in eAT with elevated eosinophils.** (A) Representative western blots of eAT showed an increase in the ratio pAKT/AKT upon insulin stimulation in HFD-fed mice that received vehicle or rIL5 for 8 weeks [n = 3–4].  $\beta$ -Actin is shown as a protein loading control. (B) Quantification of western blots revealed no difference in the eAT insulin signaling response via pAKT/AKT between vehicle and rIL5 treated mice. Data are shown as means  $\pm$  SEM. eAT = epididymal adipose tissue; HFD = high fat diet. Key: vehicle = grey; rIL5 = black; insulin injected = dotted bars; no-insulin saline control injection = open bars. \* $P < 0.05$ , compared to no insulin stimulation.

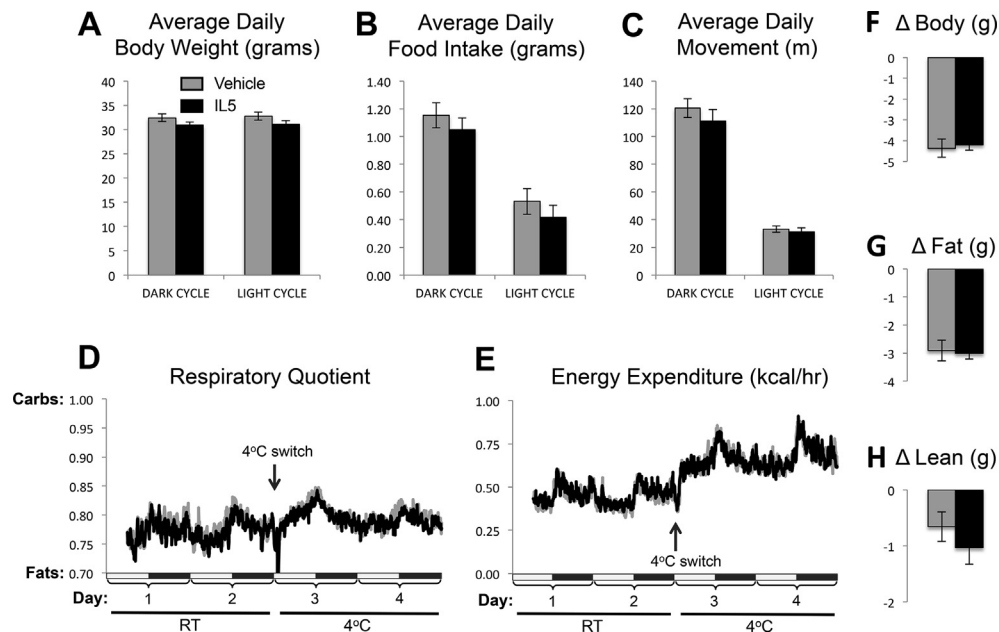


**Figure 7: Cold challenge: Energy balance in mice with elevated AT eosinophils.** HFD-fed mice that previously received vehicle or rIL5 for 8 weeks were individually housed in metabolic cages to measure an array of physiological parameters for 2 days at RT and 2 days at 4 °C [n = 8]. **(A)** Average daily body weight did not vary between vehicle and rIL5 treated mice. **(B)** Average daily food intake and **(C)** average daily movement were increased in the dark cycle compared to light cycle, but with no difference between vehicle and rIL5. **(D)** The respiratory quotient oscillated between light and dark cycles to equal degrees in vehicle and rIL5 treated mice, both during RT and the 4 °C cold challenge; indicating both groups had the same energy substrate utilization. **(E)** Energy expenditure increased upon 4 °C cold challenge to maintain body heat, but did not vary between vehicle and rIL5 treated mice. Both treatment groups lost the same amount of **(F)** body mass, **(G)** fat mass, and **(H)** lean mass. Data are shown as means  $\pm$  SEM. eAT = epididymal adipose tissue; sAT = subcutaneous AT. RT = room temperature, set at 21 °C; HFD = high fat diet. Key: vehicle = grey bars/lines; rIL5 = black bars/lines.

These findings are perplexing in light of multiple other studies that used hypereosinophilic models to improve metabolic health. While the studies summarized in the Introduction are supportive of AT being positively affected by eosinophils, subsequent publications, including our current report, have revealed that the initial understanding may be more dynamic or complex than originally appreciated. For instance, a 2014 study argued that AT eosinophils secrete IL4/IL13 to induce macrophage expression of tyrosine hydroxylase required for catecholamine production that subsequently beiges subcutaneous white AT [13]. Beiging is typically favorable because it reduces weight and inflammation, while increasing metabolic functions such as glucose tolerance and insulin sensitivity [22]. This mechanism was challenged in a multi-laboratory study providing strong evidence that macrophages are incapable of expressing tyrosine hydroxylase and therefore can't produce catecholamines to beige white AT [23], also calling into question the upstream role of eosinophils in beiging. Offering greater clarification, several studies have subsequently shown that there are nerve-associated macrophages (NAMs/SAMs) in close proximity to tyrosine-hydroxylase producing sympathetic nerves within AT [24,25]. These NAMs/SAMs were shown to take up and catabolize catecholamines produced by the nerves, effectively regulating the amount of catecholamines available to act on surrounding adipocytes. In this way, macrophages may be indirectly regulating catecholamine reserves that could otherwise beige the AT; however, it is not clear whether eosinophils interact with these NAMs/SAMs. Separately, Brestoff *et al.* showed that while ILC2s can be stimulated with IL33 to induce AT beiging, in their model this was not dependent on eosinophils or IL4 signaling [26]. Instead, their evidence suggested ILC2s acted directly on the adipocytes to increase UCP1 via methionine-enkephalin peptides. Van den Berg *et al.* showed that while helminth stimulation

induced eosinophilia in both eAT and sAT, there was no beiging in eAT and only a slight increase in sAT [27]. In our previously published work, we showed CCR2<sup>-/-</sup> mice have increased AT eosinophils but no reduction in fat mass or improved glucose tolerance [21,28]. Lastly, while previous studies have shown increased eosinophils correlated with M2-like macrophage polarization, an intriguing new study by Qin *et al.* demonstrates that eosinophils treated first with oxidized-LDL elicit M1-like macrophages [29]; suggesting that eosinophils are capable of polarizing either M1- or M2-like macrophages depending on environmental cues.

While these studies do not outright refute a role for eosinophils to positively regulate AT function and thus metabolic fitness, they do call into question the currently proposed mechanisms. Our study shows that restoring AT eosinophils in obese mice to higher levels seen in lean mice, does not improve any of a range of metabolic parameters, either at the local AT level or systemically. It is our conclusion that if eosinophils are capable of improving metabolic health via AT, increasing the number of eosinophils alone is not sufficient to drive such changes. Rather, the eosinophil phenotype and level of activation may also be playing a critically necessary role. Alternatively, it may be that increased eosinophils in a tissue besides AT are responsible for systemic metabolic improvements; indeed, to our knowledge, there have been no models that increased eosinophils exclusively in AT and subsequently showed systemic metabolic improvements. Lastly, it may have been upstream or off-target cellular/molecular targets in previous models that were responsible for metabolic improvements, instead of eosinophils that could have simply been a downstream effect. Future studies must address these possible explanations for the discrepancies between studies to more fully understand the role of eosinophils in metabolic health.

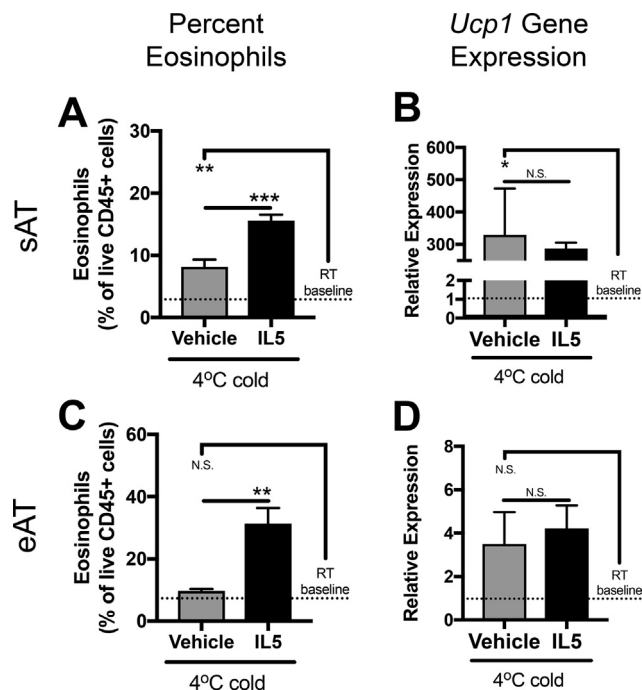


**Figure 8: Cold challenge: Being capacity of white AT with elevated eosinophils.** AT of HFD-fed mice that received vehicle or rIL5 for 8 weeks was examined after 2 days of RT or 4 °C cold exposure. After cold exposure, the presence of increased eosinophils was verified in (A) sAT and (C) eAT of rIL5 treated mice compared to vehicle controls [n = 5–7]. Cold exposure alone was able to increase eosinophils in sAT but not eAT. (B) *Ucp1* gene expression in sAT was increased ~307-fold in the cold compared to RT, with no further increase in rIL5 treated mice [n = 4–5]. (D) *Ucp1* gene expression in eAT trended towards an increase under cold conditions, but no difference was observed between vehicle and rIL5 treated mice [n = 5–7]. Data are shown as means ± SEM. eAT = epididymal adipose tissue; sAT = subcutaneous AT; RT = room temperature, set at 21 °C; HFD = high fat diet; *Ucp1* = uncoupling protein 1. Key: vehicle = grey bars; rIL5 = black bars.

## AUTHOR CONTRIBUTIONS

WRB contributed the most substantial amount of work towards the study's conception, design, and performance. KRP, MJH, AJK, MLG, and AHH also contributed to the study's conception, design, and performance. WRB, KRP, MJH, AJK, MLG, and AHH each assisted in drafting the article for submission and have approved the final version.

## ACKNOWLEDGEMENTS

This project was supported by a Merit Award from the Veterans Affairs to AHH (5I01BX002195) and by a Predoctoral Fellowship from the American Heart Association to WRB (15PRE25560126). WRB was also supported by Molecular Endocrinology Training Grant (DK07563). AHH was also supported by an Established Investigator Award from the American Heart Association (12EIA827), and by an Innovation Award from the American Diabetes Association (1-17-IBS-140). We would like to acknowledge the following Vanderbilt Core funding support:

- 1) MMPC supported by NIH grant U24 DK059637.
- 2) FCSR supported by the Vanderbilt Ingram Cancer Center P30-CA68485 and the Vanderbilt Digestive Disease Research Center DK058404.
- 3) CISR supported by NIH grants CA68485, DK20593, DK58404, DK59637 & EY08126.
- 4) HA&ASC supported by NIH grants DK059637 and DK020593.

We would like to acknowledge Elijah Trefts for his assistance with the oral gavage administration during the TG tolerance test and Dr. Louise Lantier for her assistance in analyzing data from the MMPC.

## CONFLICT OF INTEREST DISCLOSURE

The authors declare no conflict of interest.

## APPENDIX A. SUPPLEMENTARY DATA

Supplementary data related to this article can be found at <https://doi.org/10.1016/j.molmet.2017.12.004>.

## REFERENCES

- [1] Rothenberg, M.E., Hogan, S.P., 2006. The eosinophil. *Annual Review of Immunology* 24:147–174.
- [2] Hogan, S.P., Koskinen, A., Foster, P.S., 1997. Interleukin-5 and eosinophils induce airway damage and bronchial hyperreactivity during allergic airway inflammation in BALB/c mice. *Immunology & Cell Biology* 75:284–288.
- [3] Proctor, W.R., Chakraborty, M., Chea, L.S., Morrison, J.C., Berkson, J.D., Semple, K., et al., 2012. Eosinophils mediate the pathogenesis of halothane-induced liver injury in mice. *Hepatology*.
- [4] Leitch, V.D., Strudwick, X.L., Matthaai, K.I., Dent, L.A., Cowin, A.J., 2009. IL-5-overexpressing mice exhibit eosinophilia and altered wound healing through mechanisms involving prolonged inflammation. *Immunology & Cell Biology* 87: 131–140.
- [5] Robertson, S.A., Mau, V.J., Young, I.G., Matthaai, K.I., 2000. Uterine eosinophils and reproductive performance in interleukin 5-deficient mice. *Journal of Reproduction and Fertility* 120:423–432.
- [6] Gouon-Evans, V., Rothenberg, M.E., Pollard, J.W., 2000. Postnatal mammary gland development requires macrophages and eosinophils. *Development* 127: 2269–2282.
- [7] Jordan, H.E., Speidel, C.C., 1923. Blood cell formation and distribution in relation to the mechanism of thyroid-accelerated metamorphosis in the larval frog. *Journal of Experimental Medicine* 38:529–541.
- [8] MacKenzie, J.R., Mattes, J., Dent, L.A., Foster, P.S., 2001. Eosinophils promote allergic disease of the lung by regulating CD4(+) Th2 lymphocyte function. *The Journal of Immunology* 167:3146–3155.
- [9] Odemuyiwa, S.O., Ghahary, A., Li, Y., Puttagunta, L., Lee, J.E., Musat-Marcu, S., et al., 2004. Cutting edge: human eosinophils regulate T cell subset selection through indoleamine 2,3-dioxygenase. *The Journal of Immunology* 173:5909–5913.
- [10] Wu, D., Molofsky, A.B., Liang, H.E., Ricardo-Gonzalez, R.R., Jouihan, H.A., Bando, J.K., et al., 2011. Eosinophils sustain adipose alternatively activated macrophages associated with glucose homeostasis. *Science* 332:243–247.
- [11] Molofsky, A.B., Nussbaum, J.C., Liang, H.E., Van Dyken, S.J., Cheng, L.E., Mohapatra, A., et al., 2013. Innate lymphoid type 2 cells sustain visceral adipose tissue eosinophils and alternatively activated macrophages. *Journal of Experimental Medicine* 210:535–549.
- [12] Hams, E., Locksley, R.M., McKenzie, A.N., Fallon, P.G., 2013. Cutting edge: IL-25 elicits innate lymphoid type 2 and type II NKT cells that regulate obesity in mice. *The Journal of Immunology* 191:5349–5353.
- [13] Qiu, Y., Nguyen, K.D., Odegaard, J.I., Cui, X., Tian, X., Locksley, R.M., et al., 2014. Eosinophils and type 2 cytokine signaling in macrophages orchestrate development of functional beige fat. *Cell* 157:1292–1308.
- [14] Fabbiano, S., Suarez-Zamorano, N., Rigo, D., Veyrat-Durebex, C., Stevanovic Dokic, A., Colín, D.J., et al., 2016. Caloric restriction leads to browning of white adipose tissue through type 2 immune signaling. *Cell Metabolism* 24: 434–446.

- [15] Ding, X., Luo, Y., Zhang, X., Zheng, H., Yang, X., Yang, X., et al., 2016. IL-33-driven ILC2/eosinophil axis in fat is induced by sympathetic tone and suppressed by obesity. *Journal of Endocrinology* 231:35–48.
- [16] Berbudi, A., Surendar, J., Ajendra, J., Gondorf, F., Schmidt, D., Neumann, A.L., et al., 2016. Filarial infection or antigen administration improves glucose tolerance in diet-induced obese mice. *Journal of Innate Immunity* 8:601–616.
- [17] Lee, M.W., Odegaard, J.I., Mukundan, L., Qiu, Y., Molofsky, A.B., Nussbaum, J.C., et al., 2015. Activated type 2 innate lymphoid cells regulate beige fat biogenesis. *Cell* 160:74–87.
- [18] Rozenberg, P., Reichman, H., Zab-Bar, I., Itan, M., Pasmanik-Chor, M., Bouffi, C., et al., 2017. CD300f:IL-5 cross-talk inhibits adipose tissue eosinophil homing and subsequent IL-4 production. *Scientific Reports* 7:5922.
- [19] Lumeng, C.N., Bodzin, J.L., Saltiel, A.R., 2007. Obesity induces a phenotypic switch in adipose tissue macrophage polarization. *Journal of Clinical Investigation* 117:175–184.
- [20] Pfaffl, M.W., 2001. A new mathematical model for relative quantification in real-time RT-PCR. *Nucleic Acids Research* 29:e45.
- [21] Bolus, W.R., Gutierrez, D.A., Kennedy, A.J., Anderson-Baucum, E.K., Hasty, A.H., 2015. CCR2 deficiency leads to increased eosinophils, alternative macrophage activation, and type 2 cytokine expression in adipose tissue. *Journal of Leukocyte Biology* 98:467–477.
- [22] Harms, M., Seale, P., 2013. Brown and beige fat: development, function and therapeutic potential. *Nature Medicine* 19:1252–1263.
- [23] Fischer, K., Ruiz, H.H., Jhun, K., Finan, B., Oberlin, D.J., van der Heide, V., et al., 2017. Alternatively activated macrophages do not synthesize catecholamines or contribute to adipose tissue adaptive thermogenesis. *Nature Medicine* 23:623–630.
- [24] Camell, C.D., Sander, J., Spadaro, O., Lee, A., Nguyen, K.Y., Wing, A., et al., 2017. Inflammasome-driven catecholamine catabolism in macrophages blunts lipolysis during ageing. *Nature* 550:119–123.
- [25] Pirzgalska, R.M., Seixas, E., Seidman, J.S., Link, V.M., Sanchez, N.M., Mahu, I., et al., 2017. Sympathetic neuron-associated macrophages contribute to obesity by importing and metabolizing norepinephrine. *Nature Medicine*.
- [26] Brestoff, J.R., Kim, B.S., Saenz, S.A., Stine, R.R., Monticelli, L.A., Sonnenberg, G.F., et al., 2015. Group 2 innate lymphoid cells promote beiging of white adipose tissue and limit obesity. *Nature* 519:242–246.
- [27] van den Berg, S.M., van Dam, A.D., Kusters, P.J.H., Beckers, L., den Toom, M., van der Velden, S., et al., 2017. Helminth antigens counteract a rapid high-fat diet-induced decrease in adipose tissue eosinophils. *Journal of Molecular Endocrinology* 59:245–255.
- [28] Gutierrez, D.A., Kennedy, A., Orr, J.S., Anderson, E.K., Webb, C.D., Gerrald, W.K., et al., 2011. Aberrant accumulation of undifferentiated myeloid cells in the adipose tissue of CCR2-deficient mice delays improvements in insulin sensitivity. *Diabetes* 60:2820–2829.
- [29] Qin, M., Wang, L., Li, F., Yang, M., Song, L., Tian, F., et al., 2017. Oxidized LDL activated eosinophil polarize macrophage phenotype from M2 to M1 through activation of CD36 scavenger receptor. *Atherosclerosis* 263:82–91.